REPORT DOCUMENTATION PAGE

Form Approved
OMB No. 0704-0188

1. REPORT DATE *(DD-MM-YYYY)*	2. REPORT TYPE	3. DATES COVERED *(From - To)*
MAY 2013	CONFERENCE PAPER (Post Print)	DEC 2010 – NOV 2012

4. TITLE AND SUBTITLE

FAST STATISTICAL MODEL OF TIO2 THIN-FILM MEMRISTOR AND DESIGN IMPLICATION

5a. CONTRACT NUMBER
FA8750-11-2-0046

5b. GRANT NUMBER
N/A

5c. PROGRAM ELEMENT NUMBER
62788F

6. AUTHOR(S)

Miao Hu, Hai Li, and Robinson Pino

5d. PROJECT NUMBER
T2NC

5e. TASK NUMBER
PO

5f. WORK UNIT NUMBER
LY

7. PERFORMING ORGANIZATION NAME(S) AND ADDRESS(ES)

Polytechnic Institute of NYU
2 MetroTech Center
Brooklyn, NY 11201

8. PERFORMING ORGANIZATION REPORT NUMBER
N/A

9. SPONSORING/MONITORING AGENCY NAME(S) AND ADDRESS(ES)

Air Force Research Laboratory/Information Directorate
Rome Research Site/RITB
525 Brooks Road
Rome NY 13441-4505

10. SPONSOR/MONITOR'S ACRONYM(S)
AFRL/RI

11. SPONSORING/MONITORING AGENCY REPORT NUMBER
AFRL-RI-RS-TP-2013-016

12. DISTRIBUTION AVAILABILITY STATEMENT
APPROVED FOR PUBLIC RELEASE; DISTRIBUTION UNLIMITED. PA Case Number: 88ABW-2011-6302
DATE CLEARED: 5 DEC 2011

13. SUPPLEMENTARY NOTES

14. ABSTRACT
The emerging memristor devices have recently received increased attention since HP Lab reported the first TiO2- based memristive structure. As it is at nano-scale geometry size, the uniformity of memristor device is difficult to control due to the process variations in the fabrication process. The incurred design concerns in a memristor-based computing system, e.g, neuromorphic computing, can be very severe because the analog states of memristors are heavily utilized. Therefore, the understanding and quantitative characterization of the impact of process variations on the electrical properties of memristors become crucial for the corresponding VLSI designs. In this work, we examined the theoretical model of TiO2 thin-film memristors and studied the relationships between the electrical parameters and the process variations of the devices. A statistical model based on a process-variation aware memristor device structure is extracted accordingly. Simulations show that our proposed model is 3 ~ 4 magnitude faster than the existing Monte-Carlo simulation method, with only ~ 2% accuracy degradation. A variable gain amplifier (VGA) is used as the case study to demonstrate the applications of our model in memristor-based circuit designs.

15. SUBJECT TERMS
TiO2, thin-film, memristor, model

16. SECURITY CLASSIFICATION OF:			17. LIMITATION OF ABSTRACT	18. NUMBER OF PAGES	19a. NAME OF RESPONSIBLE PERSON
a. REPORT	b. ABSTRACT	c. THIS PAGE			NATHAN MCDONALD
U	U	U	UU	9	19b. TELEPHONE NUMBER (*Include area code*) N/A

Fast Statistical Model of TiO_2 Thin-Film Memristor and Design Implication

Miao Hu
Dept. of ECE
Polytechnic Institute of NYU
Brooklyn, NY, USA
Email: mhu01@students.poly.edu

Hai Li
Dept. of ECE
Polytechnic Institute of NYU
Brooklyn, NY, USA
Email: hli@poly.edu

Robinson E. Pino
Air Force Research Laboratory
Advanced Computing
Rome, NY, USA
Email: robinson.pino@rl.af.mil

***Abstract*—The emerging memristor devices have recently received increased attention since HP Lab reported the first TiO_2-based memristive structure. As it is at nano-scale geometry size, the uniformity of memristor device is difficult to control due to the process variations in the fabrication process. The incurred design concerns in a memristor-based computing system, e.g, neuromorphic computing, can be very severe because the analog states of memristors are heavily utilized. Therefore, the understanding and quantitative characterization of the impact of process variations on the electrical properties of memristors become crucial for the corresponding VLSI designs. In this work, we examined the theoretical model of TiO_2 thin-film memristors and studied the relationships between the electrical parameters and the process variations of the devices. A statistical model based on a process-variation aware memristor device structure is extracted accordingly. Simulations show that our proposed model is $3 \sim 4$ magnitude faster than the existing Monte-Carlo simulation method, with only $\sim 2\%$ accuracy degradation. A variable gain amplifier (VGA) is used as the case study to demonstrate the applications of our model in memristor-based circuit designs.**

I. Introduction

Based on the completeness of circuit theory, Prof. Chua predicted the existence of the fourth fundamental passive circuit element – memristor in 1971 [1]. Till 2008, a real memristor device was implemented through a TiO_2 thin-film structure [2]. Since then, many different types of memristor materials and devices have been reported or rediscovered.

Memristors show many promising characteristics as the next-generation data storage devices, such as non-volatility, low-power consumption, high integration density and excellent scalability [3][4]. Also, the special property that *remembers* historical profile of the electrical excitations on the device [5] makes memristor an ideal candidate to realize the synapse behavior in electronic neural networks [6][7].

As process technology scales down to 45nm and below, process variations, e.g., line-edge roughness (LER), oxide thickness fluctuation (OTF), and random discrete doping (RDD) [8], lead to significant device parameter fluctuations. The impact of process variations on a memristive system may be more severe than a conventional digital design because of the utilization of the analog states of memristors. Many models have been carried out for various memristor devices, including TiO_2 thin-film memristors [9], spintronic memristors [10], and ion conductor chalcogenide-based memristors [11]. Very recently, Hu *et al.* presented a geometry-variation aware memristor device structure model [12]. The associated Monte-Carlo simulation flow, however, is very time-consuming.

In this work, we developed a fast statistical model to simulate the electrical properties of TiO_2 thin-film memristors. Starting with the theoretical model of a TiO_2 thin-film memristor, we explored the influences of geometry variations on the electrical parameters of the device. On top of that, a statistical model with the merits of both high accuracy and low runtime cost is proposed. Compared to the existing work in [12], our model significantly improves the runtime cost by $3 \sim 4$ orders of magnitude; and reduces the input data set down to a few variables. The simulation accuracy maintains within $\sim 2\%$ discrepancy in the whole working region of the memristor device, compared to the results using the model in [12]. Furthermore, we demonstrated a design example – an op-amp based variable gain amplifier (VGA), and analyzed the impact of process variations to the design with the extracted statistical model.

The rest of paper is organized as follows: Section II introduces the memristor basics, including the theory and the physical mechanisms of TiO_2 thin-film memristors, and analyzes the impact of process variations on the device electrical properties; Section III illustrates the theoretical fundamentals of our proposed model; Section IV explains the methodology to generate our proposed statistical model; Section V demonstrates the effectiveness and accuracy of our proposed model by some examples; and Section VI concludes our work.

II. Background

A. Memristor Theory

The original definition of the memristor is derived from the completeness of circuit theory: besides resistor, capacitor and inductor, there exists the fourth basic two-terminal element that uniquely defines the relationship between the magnetic flux (φ) and the electric charge (q) passing through the device, or $d\varphi = M \cdot dq$ [1]. Since $\varphi = \int V dt$ and $q = \int I dt$, the definition of the memristor can be generalized as:

$$\begin{cases} V = M(\omega, I) \cdot I \\ \frac{d\omega}{dt} = f(\omega, I) \end{cases}, \quad (1)$$

978-1-4577-1400-9/11/$26.00 ©2011 IEEE

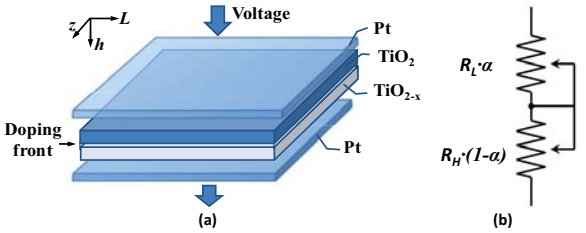

Fig. 1. TiO_2 thin-film memristor. (a) structure, and (b) equivalent circuit.

where ω is a state variable; $M(\omega, I)$ denotes the instantaneous memristance, which may vary over time. Under certain conditions, $M(\omega, I)$ and $f(\omega, I)$ may be simplified as the explicit functions of I.

B. TiO_2 Memristor

In 2008, HP Lab demonstrated the memristive effect by moving the doping front along a TiO_2 thin-film [2]. Fig. 1(a) illustrates the Pt/TiO_2/Pt structure. The stoichiometric TiO_2 with exactly 2:1 ratio of oxygen to titanium has a low conductivity and can be considered as an insulator. When the TiO_2 loses a certain amount of oxygen (called oxygen-deficient titanium dioxide), its conductivity becomes relatively high as a semiconductor. A positive bias causes the oxygen vacancies to drift to the pure TiO_2 region and lowers the overall resistance continuously. A negative bias, however, reverses the above process and raises the overall resistance [3].

Fig. 1(b) illustrates the equivalent circuit of such a TiO_2 thin-film memristor as two resistors connected in series. R_L (R_H) denotes the lowest (highest) resistance of the device when the memristor is fully doped or undoped, respectively. The total memristance of a TiO_2 memristor can be expressed as

$$M(\alpha) = R_L \cdot \alpha + R_H \cdot (1 - \alpha). \tag{2}$$

Here α ($0 \leq \alpha \leq 1$) is the relative doping front position, which is the ratio of doping front position over the total thickness of the TiO_2 thin-film.

The velocity of doping front movement $v(t)$, which is driven by the voltage applied across the memristor $V(t)$ can be expressed as

$$v(t) = \frac{d\alpha}{dt} = \mu_v \cdot \frac{R_L}{h^2} \cdot \frac{V(t)}{M(\alpha)}, \tag{3}$$

where μ_v is the equivalent mobility of dopants; h is the thickness of the TiO_2 thin film; and $M(\alpha)$ is the total memristance when the relative doping front position is α. The change of α over time t can be obtained by solving the differential equation Eq. (3) as

$$\alpha(t) = \frac{R_H - \sqrt{R_H^2 - 2 \cdot (R_H - R_L) \cdot (A + B)}}{R_H - R_L}. \tag{4}$$

Here $A = \mu_v \cdot \frac{R_L}{h^2} \cdot \int_{t_0}^{t} V(t)dt$ exhibits the memristor's historic behavior; and $B = R_H \cdot \alpha_0 + \frac{1}{2} \cdot (R_L - R_H) \cdot \alpha_0^2$ is determined by the initial condition $\alpha_0 = \alpha(t_0)$.

C. Process-Variation Aware Monte-Carlo Simulations

The process variations significantly influence the electrical properties of nano-devices. For a TiO_2 thin-film memristor, there are three major sources of process variations: (1) Line edge roughness (LER), which is generated in the lithography and etching steps and causes the deviation of the printed image's edge from its designed pattern; (2) Oxide thickness fluctuation (OTF), which is generated in the deposition process; and (3) Random discrete doping (RDD), which leads to the material non-uniformity within the device. In the rest of paper, without loss of generality, we use ω and ω' to respectively represent the design value and the actual value under process variations for any given variable ω.

Very recently, a Monte-Carlo simulation method was proposed to analyze the impact of geometry variations on the electrical properties of TiO_2 thin-film memristors [12]. A 3D device structure including the geometry variation information is generated by performing a sanity check of the device characterization parameters. In the Monte-Carlo simulations, the memristor device is divided into many small filaments sandwiched between two electrodes. Within a filament i, the cross-section area $s'_i = l'_i \cdot z'_i$ and thickness h'_i, can be considered as constants, whose value can be modeled by taking into account the effects of LER or OTF, respectively. The corresponding memristance and doping front position of filament i can be represented as

$$M'_i(\alpha) = R'_{L,i} \cdot \alpha'_i + R'_{H,i} \cdot (1 - \alpha'_i), \tag{5}$$

and

$$\alpha'_i(t) = \frac{R'_{H,i} - \sqrt{R'^2_{H,i} - 2 \cdot (R'_{H,i} - R'_{L,i}) \cdot (A'_i + B'_i)}}{R'_{H,i} - R'_{L,i}}, \tag{6}$$

where the coefficients $A'_i = \mu_v \cdot \frac{R'_{L,i}}{h'^2_i} \cdot \int_{t_0}^{t} V(t) \cdot dt$ and $B'_i = R'_{H,i} \cdot \alpha_0 + \frac{1}{2}(R'_{L,i} - R'_{H,i}) \cdot \alpha_0^2$.

The two boundary resistances of filament i: $R'_{L,i}$ and $R'_{H,i}$, which can be calculated by

$$R'_{L,i} = \int_0^{h'_i} \frac{\rho_{on}}{s'_i(\alpha'_i)} \cdot d\alpha'_i, \tag{7}$$

and

$$R'_{H,i} = \int_0^{h'_i} \frac{\rho_{off}}{s'_i(\alpha'_i)} \cdot d\alpha'_i. \tag{8}$$

vary from filament to filament under the process variations. Here ρ_{on} and ρ_{off} are the electrical resistivity of the doped and updoped TiO_2 thin-film, respectively, which suffer from the RDD issue.

The overall instantaneous memristance of the TiO_2 memristor can be calculated as the total resistance of all n filaments connected in parallel as

$$M'(t) = \frac{1}{\sum_{i=1}^{n} 1/M'_i}. \tag{9}$$

Due to the thin film thickness fluctuation (and/or the roughness of the electrode contact), the doping front movement inside every filament varies. Therefore, a concept named "average doping front position" is introduced as

$$\alpha'(t) = \frac{R'_H - M'(t)}{R'_H - R'_L}. \tag{10}$$

In the Monte-Carlo simulation flow proposed in [12], a filament based process variation model is carried out. However, due to its large runtime cost, this technique is infeasible in large scale circuit and system designs. In this work, we will proposed a more efficient process-variation aware memristor model with a very slight accuracy relaxation.

III. An Analysis Of Memristor Model

Compared to other fundamental passive devices, the modeling of memristors has some unique challenges: First, as a time-varying device whose properties are determined by the historic profile of electrical excitations, not only the variations of the start and the end states, but also that of the intermediate time-varying state must be modeled; Second, as an analog device that can be used in diverse circuit styles and environments, various device properties, e.g., the total memristance and its changing rate, the timing and frequency responses, and I-V characteristic, must be modeled; finally, the calibration and validation of the proposed models can be challenging due to the lack of published measurement data.

When the device variations are within the reasonable range, we can assume the ratio between the actual device parameter and its designed value as a polynomial expression, or $x' = \eta \cdot x$. Here η is a coefficient representing the effects of process variations. Our goal is to find an efficient methodology to compute the variation-aware coefficient η.

The total memristance M', which is a time-varying parameter, can be uniquely defined by R'_H, R'_L, and $\alpha'(t)$. In this section, we will examine the variations of R'_H, R'_L, and $\alpha'(t)$ first, and then derive the corresponding process-variation aware memristance model. Table I summarizes the designed values of the TiO_2 memristor geometry dimensions and its electrical parameters adopted in our work [2].

A. Distribution of R'_H and R'_L

For a given TiO_2 memristor, we use R'_H and R'_L to denote its actual highest and lowest total memristances, respectively. As Eq. (7) and (8), the geometry variations (h'_i and s'_i) influence both $R'_{H,i}$ and $R'_{L,i}$ simultaneously within the filament i. It indicates $R'_{H,i}$ and $R'_{L,i}$ are correlated. However, they are not fully correlated because of the randomness in ρ_{off} and ρ_{on}, which is incurred by RDD. We define $\gamma = \rho_{off}/\rho_{on}$ to describe the RDD effect, which can be modeled by a normal distribution as $\gamma' = \mu_\gamma \cdot (1 + \sigma_\gamma \cdot D)$. Here $\mu_\gamma = R_H/R_L$ and $D \sim \mathcal{N}(0,1)$. The actual value of σ_γ will be determined by the particular device structure, material and fabrication process. In our following simulations, we assume $\sigma_\gamma = 2\%$.

To obtain the distributions of R'_H and R'_L, we conducted Monte-Carlo simulations with 10,000 3D device samples. The variation samples are generated by the same algorithm and constraints in [12]. Our results show that the distributions of both R'_H and R'_L are close to normal distributions and can be approximated by

$$R'_L = R_L \cdot (\mu_{R_L} + \sigma_{R_L} \cdot E), \tag{11}$$

and

$$R'_H = R_H \cdot (\mu_{R_H} + \sigma_{R_H} \cdot E) \cdot (1 + \sigma_\gamma \cdot D). \tag{12}$$

Here, two independent random numbers $E \sim \mathcal{N}(0,1)$ and $D \sim \mathcal{N}(0,1)$ are introduced. E represents the correlation between R'_H and R'_L due to the same geometry variation sources. D represents the impact of RDD, which affects the ratio between ρ_{off} and ρ_{on}.

TABLE I
The Ideal Parameters of a TiO_2 Thin-film Memristor.

Geometry Dimensions		Electrical Parameters	
Length (l)	50 nm	R_H	16,000 Ω
Width (w)	50 nm	R_L	100 Ω
Thickness (h)	50 nm	μ_v	$10^{-14}\ m^2 S^{-1} V^{-1}$

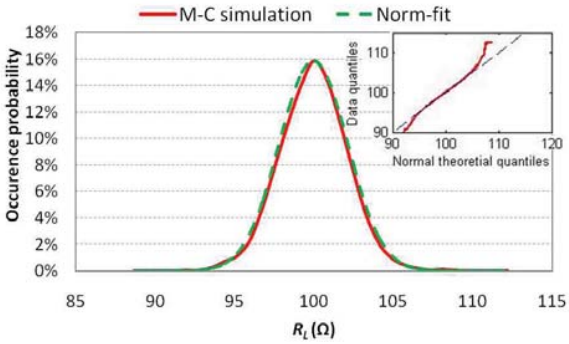

Fig. 2. The Distribution of R'_L from 10,000 Monte-Carlo simulations and the fitting curve of Eq. (11).

Fig. 2 compares the approximated normal distribution shown in Eq. (11) and the actual distribution of R'_L from Monte-Carlo simulations. The root mean square error (RMSE) incurred by the normal distribution approximation is only 4.4%. A quantile-quantile plot is also shown in the inset of the figure.

B. Distribution of α'

As shown in Eq. (10), the calculation of the average doping front α' requires time-consuming filament-based simulations. If we can somehow extract the actual α' directly from the designed value α by using a simplified process variation model, the simulation cost can be improved.

Considering the fact that $R_H \gg R_L$ in a TiO_2 memristor, a simple approximation of Eq. (4) can be:

$$\alpha(t) = 1 - \sqrt{1 - X}, \tag{13}$$

where,

$$X = \frac{2\mu_v}{\gamma \cdot h^2} \cdot \left(\int_{t_0}^{t} V(t) \cdot dt + \alpha_0 - \frac{1}{2} \cdot \alpha_0^2\right). \tag{14}$$

Eq. (14) shows that the variation of α can be directly linked to the variation of X, which has three independent contributors: (1) the variation of thin-film thickness h, (2) the impact of RDD that is represented by γ, and (3) the magnetic flux of the input signal $\varphi = \int V dt$. Interestingly, LER does not impact α', as also proved by the simulations in [12].

Impact of flux φ and boundary conditions.

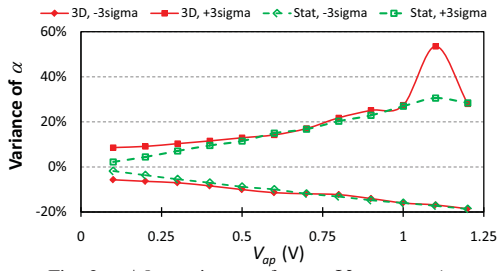

Fig. 3. $\pm 3\sigma$ variances of α vs. V_{ap} at $t = 1s$.

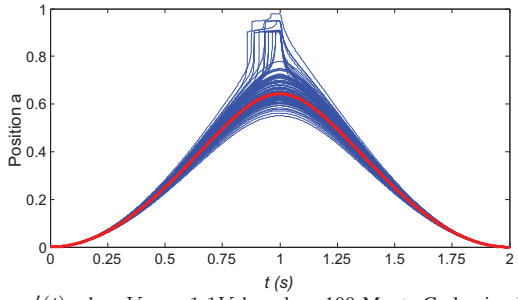

Fig. 4. $\alpha'(t)$ when $V_{ap} = 1.1V$ based on 100 Monte-Carlo simulations.

If there are no process variations, the average doping front α will be uniquely determined by the magnetic flux φ, as shown in Eq. (14). However, when process variations are considered, the historical profile of the electrical excitations (instead of only the absolute value of φ) will introduce the additional variations of φ by interacting with the device variations such as thin film thickness h' and RDD γ'.

To understand how the historical profiles of φ, e.g., the amplitude and the time duration etc., affect the variation of α, we conducted the Monte-Carlo simulations with 10,000 3D device samples and traced the doping front the position $\alpha'(t)$ in every device samples. A sinusoid input signal $V = V_{ap} \cdot \sin(2\pi f \cdot t)$ with a fixed frequency $f = 0.5Hz$ is applied. The $+3\sigma$ and -3σ variations of $\alpha(t = 1s)$, which has been normalized against the designed value of $\alpha(t = 1s)$ when varying V_{ap} from $0.1V$ to $1.2V$, are shown as the curves labeled with "3D, +3sigma" and "3D, -3sigma" in Fig. 3, respectively. Here $\varphi(t = 1s) = V_{ap}/(\pi f)$, which is proportional to V_{ap}.

The simulation results show that the 3σ variance of α' is approximately proportional to φ, except when α' is close to 1 (or the total memristance is close to R'_L). A significant overshoot of the $+3\sigma$ variance at $V_{ap} = 1.1V$ is observed. Based on the mathematic expression in Eq. (13–14), it indicates that α has a wider distribution when X is approaching 1.

A closer look of this boundary situation is shown in Fig. 4. It records the movement history of the doping fronts of 100 device samples when $V_{ap} = 1.1V$. The RED curve is the designed behavior while the 100 BLUE curves come from Monte-Carlo simulations. The average doping fronts of some devices with large process variations hit the device boundary during the movements and cause the large variance of α' at the $+3\sigma$ corner. However, large α' variance at the -3σ corner not observed in Fig. 3. It is because the average doping front of the most devices at the -3σ corner will not reach the device boundary under the simulated electrical excitations.

TABLE II
STATISTICAL MODEL OF TiO_2 THIN-FILM MEMRISTOR.

Variation Parameters: μ_{R_H}, σ_{R_H}, μ_{R_L}, σ_{R_L}, σ_γ
Coefficients: w_1, w_2, ε_1, ε_2
Independent Random Numbers:
$D \sim \mathcal{N}(0,1)$, $E \sim \mathcal{N}(0,1)$, $G \sim \mathcal{N}(0,1)$.
Memristance boundary:
$R'_H = R_H \cdot (\mu_{R_H} + \sigma_{R_H} \cdot E) \cdot (1 + \sigma_\gamma \cdot D)$
$R'_L = R_L \cdot (\mu_{R_L} + \sigma_{R_L}) \cdot E$
Input flux:
$$\varphi_{eff} = \begin{cases} \int_{t_0}^{t} V_{ap} \cdot dt & (\alpha' < 1) \\ h^2(R_H + R_L)/(2\mu_v R_L) & (\alpha' \geq 1) \end{cases}$$
Doping front position:
$\alpha' = \eta \cdot \alpha$
$\eta = \frac{1}{(1+\varphi\cdot\varepsilon_1+\varphi\cdot\varepsilon_2\cdot(w_1\cdot E+w_2\cdot G))\cdot(1+\sigma_\gamma\cdot D)}$
Memristance:
$M'(\alpha) = R'_L \cdot \alpha' + R'_H \cdot (1 - \alpha')$

Further increasing the flux φ, i.e., increasing V_{ap} from $1.1V$ to $1.2V$ makes the variance of α' drop, as also shown in Fig. 3. Under this scenario, the amplitude of φ is so large that the average doping front of the most simulated devices have reached the device boundary. These devices have a constant $\alpha' = 1$ and therefore, will not contribute to the variances of average doping fronts. A new concept named "effective flux," which includes the constraints of device boundary, can be expressed as

$$\varphi_{eff} = \begin{cases} \int_{t_0}^{t} V_{ap} \cdot dt & (\alpha' < 1) \\ h^2(R_H + R_L)/(2\mu_v R_L) & (\alpha' \geq 1). \end{cases} \quad (15)$$

Impact of process variations.

The complexity of Eq. (13) and (14) make it infeasible to derive a simple analytical expression of the variance of α' even if we assume both h' and γ' follow normal distributions. However, we are still able to construct a polynomial-based α' model to approximate the variations of the average doping front in the memristor device.

By running extensive numerical simulations under various conditions, we found the actual α' can be modeled as the product of the designed value α and a coefficient η that represents the influence of process variations as:

$$\alpha' = \eta \cdot \alpha. \quad (16)$$

Here η can be expressed by a heuristic formula (partially from the first order Taylor expansion of Eq. (13) and (14)) as

$$\eta = \frac{1}{(1+\varphi\cdot\varepsilon_1+\varphi\cdot\varepsilon_2\cdot(w_1\cdot E+w_2\cdot G))\cdot(1+\sigma_\gamma\cdot D)}. \quad (17)$$

Similar to the definitions we used in Section III-A, D and E are two independent random numbers that represent the impact of the RDD and the geometry variations, respectively. To avoid overestimating the impact of geometry variations on α', a new random number $G \sim \mathcal{N}(0,1)$ is introduced to offset the impact of LER. ε_1 and ε_2 are two scalars extracted from the actual simulations. The coefficients w_1 and w_2 represent the weights of E and G, where $w_1^2 + w_2^2 = 1$.

C. Distribution of M′

By modeling R'_L, R'_H and α' with Eq. (11) (12) (16), the total memristance M' of a TiO_2 memristor can be simply calculated by Eq. (2), where the design values of R_H/R_L and α should be replaced by the actual values R'_H, R'_L and α'. Table II summarizes the main steps and equations included in our proposed statistical model of TiO_2 memristors.

IV. Model Generation Flow

In this section, we describe the methodology to extract the parameters included in our proposed statistical model of TiO_2 memristors. Some critical implementation considerations are also discussed.

A. Parameter Extraction

Based on the discussion in Section III, we proposed a four-step extraction methodology to obtain the parameters required by our proposed statistical model.

Step 1: Model input characterization.

In the electrical testing of a memristor device, only three parameters can be measured directly: R'_H, R'_L and $I(t)$(or$V(t)$. The measurement of $I(t)$, which is a time-varying variable, requires two doping front α movements following $0 \rightarrow 1$ and $1 \rightarrow 0$ directions under certain electrical excitations: as we discussed in Section III-B, the electrical excitations must be carefully controlled to prevent the doping front from hitting the boundaries. The absolute value of the flux φ can be simply calculated as the integral of the applied voltage over time.

Step 2: Distribution generations for R'_H and R'_L.

The PDF of R'_L can be modeled as a normal distribution as shown in Eq. (11). The mean μ_{R_L} and the variance σ_{R_L} can be easily extracted from the statistical data measured (or simulated if Monte-Carlo simulation is used) in Step 1. Though R'_H does not strictly follow a normal distribution in Eq. (12), a mean of μ_{R_H} can still be extracted. Since being exposed to the same geometry variations, $\sigma_{R_H} \approx \sigma_{R_L}$ in Eq. (12). As we shall show in Section V-A, modeling R'_H as a normal distribution approximation introduces very marginal discrepancies from the statistical data and incurs very little impact on the accuracy of α modeling. Finally, the variance of σ_γ needs to be provided by material-level characterizations.

Step 3: Distribution generation for α'.

For every memristor sample, the total memristance and their average doping front position at a given time stamp t_j can be calculated as:

$$M'(t_j) = \frac{V(t_j)}{I(t_j)},\ \alpha'(t_j) = \frac{R'_H - M'(t_j)}{R'_H - R'_L}. \tag{18}$$

Monte-Carlo simulations can derive the distribution of $M'(t_j)$ and $\alpha'(t_j)$ and the mean μ_α and the variance σ_α of $\alpha'(t_j)$. Then two scalars – ε_1 and ε_2 can be extracted by Eq. (16) and (17) with estimation method.

We proposed a heuristic method to generate w_1 and w_2: We start with an assumption that $w_1 = 1$ and $w_2 = 0$. The derived mean μ_M and variance σ_M of total memristance M are then compared to the corresponding parameters of the measured data M', say, $\mu_{\hat{M}}$ and $\sigma_{\hat{M}}$. If the impact of geometry variations is overestimated, we will have $\sigma_{\hat{M}} > \sigma_M$ and $\mu_{\hat{M}} \neq \mu_M$. We then adjust the values of w_1 and w_2 to reduce the mismatch. The optimal approximations of w_1 and w_2 can be obtained when the parameter mismatch is below an acceptable threshold.

Step 4: Model verification and improvement.

The above parameters only take a few minutes to be extracted when sufficient data provided and sophisticated estimation method applied. After all necessary parameters are extracted, the statistical models can be constructed. The static and dynamic behaviors of TiO_2 memristors under various electrical excitations can be simulated by our model without conducting the time-consuming Monte-Carlo simulations. The accuracy of our proposed model can still be verified by comparing to the Monte-Carlo simulation results. The accuracy of our proposed model could be improved by optimizing the iteration termination conditions of the parameter extraction processes.

B. Flow Summary

The pseudocode of the simulation flow of the memristor dynamic behavior is summarized below:

Algorithm 1: Statistical Model for Computer Simulation

$E = \mathcal{N}(0,1)$, $G = \mathcal{N}(0,1)$, $D = \mathcal{N}(0,1)$ generated at the beginning of simulation;

$\varphi(n+1) = \varphi(n) + V(n+1) \cdot dt$
if $abs(\varphi(n+1)) > \varphi_{eff}$
  $\varphi(n+1) = sign(\varphi(n+1)) \cdot \varphi_{eff}$
end if
$\eta(n+1) = \frac{1}{(1+\varphi(n+1)\cdot\varepsilon_1+\varphi(n+1)\cdot\varepsilon_2\cdot(w_1\cdot E+w_2\cdot G))\cdot(1+\sigma_\gamma\cdot D)}$
$vel(n+1) = \mu_v \cdot \frac{R_L}{h^2} \cdot \frac{V(n+1)}{M(n)}$
$\alpha(n+1) = a(n) + vel(n+1) \cdot dt$
$\alpha'(n+1) = \eta(n+1) \cdot \alpha(n+1)$
Check boundary condition of $\alpha'(n+1)$
If $\alpha'(n+1)$ reaches boundary
$\varphi(n+1) = 0$
end if
$M'(n+1) = R'_L \cdot \alpha'(n+1) + R'_H \cdot (1 - \alpha'(n+1))$
return M

V. Model verification and design implication

A. Model Verification

Because of the lack of published data on memristor device variations, we use Monte-Carlo simulation results as our baseline to validate the proposed statistical model. Three basic memristor testing data – R'_H, R'_L and $I(t)$, are generated from the simulations on the 3D device structure examples generated

TABLE III
Statistical model parameters

Variation Parameters		Coefficients	
μ_{R_H}	0.994	ε_1	-0.028
μ_{R_L}	0.994	ε_2	0.072
σ_{R_H}	2.16%	w_1	0.98
σ_{R_L}	2.16%	w_2	0.2
σ_γ	2%		

TABLE IV
Variance between 3D model and statistical model.

	$a-t$	$M-t$	$V-I$
$+3\sigma$	4.97%	2.03%	2.20%
-3σ	5.05%	2.12%	1.99%

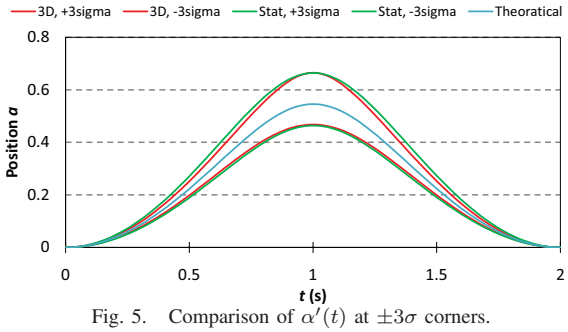

Fig. 5. Comparison of $\alpha'(t)$ at $\pm 3\sigma$ corners.

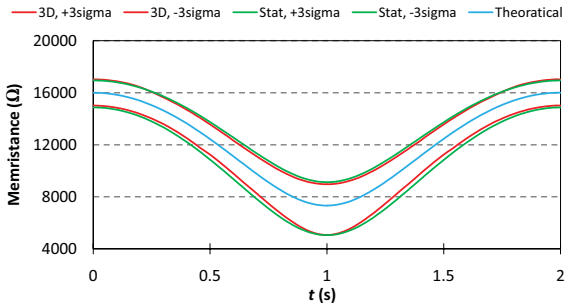

Fig. 6. Comparison of $M'(t)$ at $\pm 3\sigma$ corners.

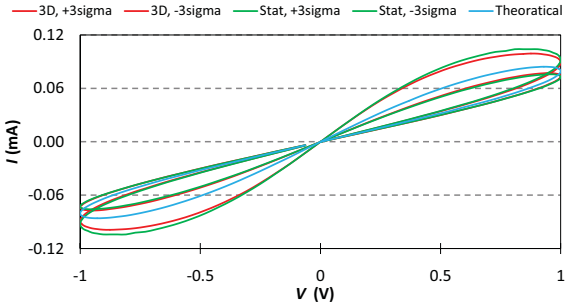

Fig. 7. Comparison of $I - V$ at $\pm 3\sigma$ corners.

by the technique in [12]. However, there is nothing preventing us from using the measurement data the input of our model generation. The parameters of the generated statistical model are summarized in TABLE III, which are used in our following simulations.

In this section, the effectiveness of our proposed statistical model is validated by comparing our simulation results of the different electrical properties of a TiO_2 memristor with that from the Monte-Carlo simulations based on 3D device structure samples. Every Monte-Carlo simulation run include 10,000 samples.

Test 1: Fixed Input Signal. A sinusoid input signal $V = V_{ap} \cdot \sin(2\pi f \cdot t)$ with $V_{ap} = 1V$ and $f = 0.5Hz$ is applied to the simulated memristor device. Fig. 5, 6, and 7 show the simulation results of $\alpha'(t)$, $M'(t)$, and $I - V$ characteristics, respectively. The results of our statistical model (labeled "stat") are very close to the results of the Monte-Carlo simulations with 3D device samples (labeled "3D"). For example, compared to 3D Monte-Carlo simulations, our memristance results shows only $\sim 2\%$ discrepancy over the simulated time range at the $\pm 3\sigma$ corners. Table IV summarizes the variances of each electrical property at each corner.

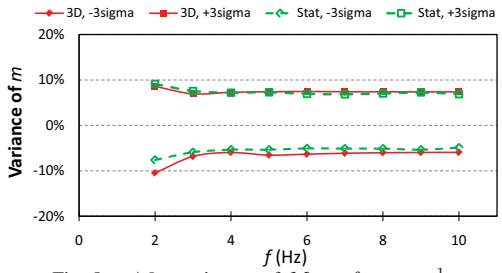

Fig. 8. $\pm 3\sigma$ variances of M vs. f at $t = \frac{1}{2f}$.

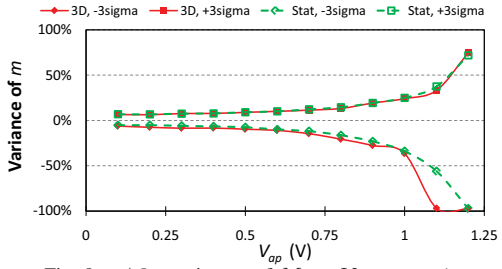

Fig. 9. $\pm 3\sigma$ variances of M vs. V_{ap} at $t = 1s$.

Test 2: Frequency Dependency. The same sinusoid input signal is applied with $V_{ap} = 2V$ while f changes from $2Hz$ to $10Hz$. Again, our statistical model demonstrates a good approximation over the whole range, as shown in Fig. 8.

Test 3: Impact of Flux. In this test, we keep the input as a sinusoid signal with a fixed $f = 0.5Hz$. We vary V_{ap} from 0.1V to 1.2V and measure α and M at $t = 1s$. For an ideal device without any process variations, α reaches to 1 when $V_{ap} = 1.26V$, which is the upper bound of our simulation. The corresponding α and M at different V_{ap}'s are shown in Fig. 3 and Fig. 9, respectively. Results show that our statistical model fits the Monte-Carlo simulation results very well except when V_{ap} is $\sim 1.1V$. The reason has been explained in Section III-B. In memristor-based analog circuit design, we recommend not to operate the memristors in this region where the doping fronts in some memristors may hit the device boundary under the process variations.

Runtime Comparison. The proposed statistical model of TiO_2 memristors significantly improves runtime cost: 10,000 device-based Monte-Carlo simulations [12] took $\sim$ 2 hours in a MATLAB environment, while the same number of simulations only took $\sim$ 2 seconds by using our proposed statistical model.

B. Applications

The statistical TiO_2 memristor model can be used to analyze the impact of process variations on memristor-based circuit designs. In this section, we use an op-amp based variable gain amplifier (VGA) [13][14] as the example to demonstrate the effectiveness of our model.

1) An op-amp based VGA with one memristor: Fig. 10 shows a simple VGA design which includes an op-amp, a resistor and a memristor [13]. V_{BIAS} is the signal to control the memristor programming. The VGA gain (G), which is the ratio between the output signal V_{OUT} and the input signal V_{IN}, is mainly determined by the memristance R_M and the

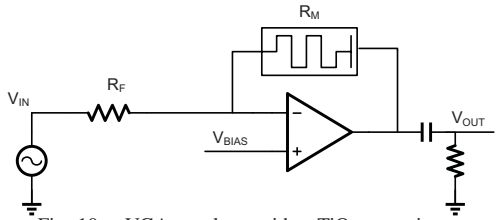

Fig. 10. VGA topology with a TiO_2 memristor.

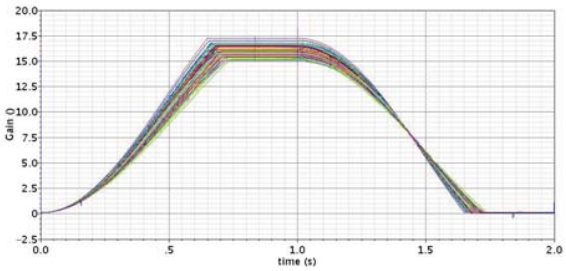

Fig. 11. Series of 100 Monte-Carlo simulations of the gains of the op-amp based VGA with one memristor.

resistance R_F as:

$$G = -\frac{V_{OUT}}{V_{IN}} = \frac{R_M}{R_F}. \quad (19)$$

In our simulation, we set the resistor $R_F = 1K\Omega$. The memristance (R_M) of an ideal memristor device sweeps from $R_L = 100\Omega$ to $R_H = 16K\Omega$. The initial state of the memristor is R_L, at which the domain wall is at the position of $\alpha = 1$. A low-frequency sinusoidal signal $V_{BIAS} = 0.2V \cdot \sin(2\pi \cdot 0.5 \cdot t)$ is applied to control the memristance of the memristor. V_{BIAS} was carefully selected in order to drive the doping front α over the full range $[0, 1]$ and demonstrate the impact of boundary conditions.A high-frequency sinusoidal signal $V_{IN} = 0.1V \cdot \sin(2\pi \cdot 1K \cdot t)$ is applied to measure G. 100 Monte-Carlo simulations are run based on our statistical TiO_2 memristor model.

Fig. 11 shows the VGA gains from the Monte-Carlo simulations. During the first half period $t = 0s \sim 1s$, V_{BIAS} is positive. G grows as R_M increases until the domain wall hits the boundary ($\alpha = 0$). In contract, a negative V_{BIAS} results in the decreases of R_M and G. As expected, the variation of G agrees with the distribution of memristance. For example, the $\pm 3\sigma$ of G at $t = 1s$ is $\sim \pm 7\%$, which is consistent with $\pm 3\sigma$ variance of the R'_L distribution shown in Fig. 2.

An interesting phenomenon observed in Fig. 11 is: during the two periods that the memristance increases and decreases, the variation of G shows the different trends. For instance, the VGA has the same μ_G at $t = 0.6s$ and $t = 1.25s$. However, $\sigma_{G(t=1.25s)}$ is much less than $\sigma_{G(t=0.6s)}$. The explanation is the follows: when programming memristor, the memristance changing rate of the memristors with high total memristance is faster than the one of the memristors with low total memristance. Such mechanism spreads the distribution of instantaneous memristance M when programming M to high and suppresses M distribution when programming M to low.

2) An op-amp based VGA with two memristors: We can replace the resistor R_F in Fig. 10 with another memristor to achieve more programming capability in VGA designs. If we

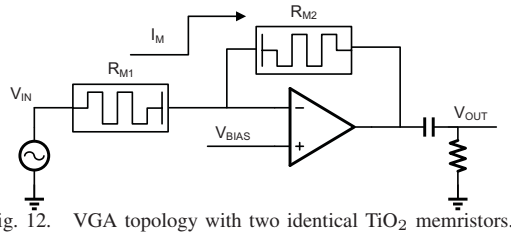

Fig. 12. VGA topology with two identical TiO_2 memristors.

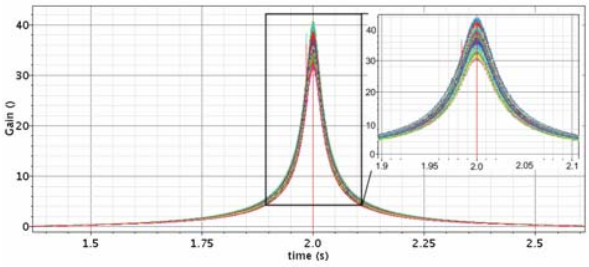

Fig. 13. Series of 100 Monte-Carlo simulations of the gains of the op-amp based VGA with two memristors.

connect the two memristors in the same direction, say, the TiO_2 portion of one memristor is connected to the TiO_{2-x} portion of the other one, the changes of their memristances will follow the same trend. Ideally, the gain of the VGA (G) will keeps constant since the ratio of the two memristances doesn't change. To obtain a wide programmable gain range of the VGA, two memristors are connected back to back as shown in Fig. 12.

We conducted Monte-Carlo simulations with the statistical TiO_2 memristor model by assuming R_{M1} and R_{M2} have the same design parameters. In the simulation, we use the same input signal V_{IN} as the previous design, and change the amplitude of the control signal V_{BIAS} to $1V$ in order to excise two memristors. The G changes over time when R_{M1} and R_{M2} are fully uncorrelated is demonstrated in Fig. 13. The input signal V_{IN}, the control signal V_{BIAS}, the current through the memristors I_M, and the output signal V_{OUT} are shown in Fig. 14. Compared to the VGA with one memristor, the range of the programmable gain G of the VGA with two memristors is significantly increased. following with the increase in G variation: $+3\sigma_{G(t=2s)} = 22.4\%$ and $-3\sigma_{G(t=2s)} = 15.5\%$.

Considering that the two memristors are made by the same process at the same time, there must be some correlations between R_{M1} and R_{M2}. Fig. 15 shows $\pm 3\sigma_G$ by adjusting the correlation coefficient of the two memristors from 0 to 1. As

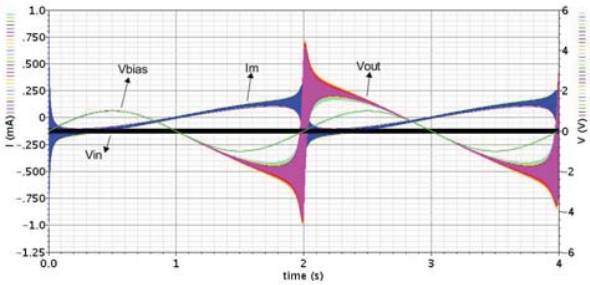

Fig. 14. Series of 100 Monte-Carlo simulations of the corresponding signals of the op-amp based VGA with two memristors.

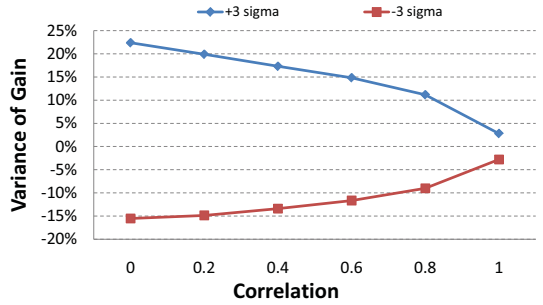

Fig. 15. The impact of device correlation on the variance of VGA gain.

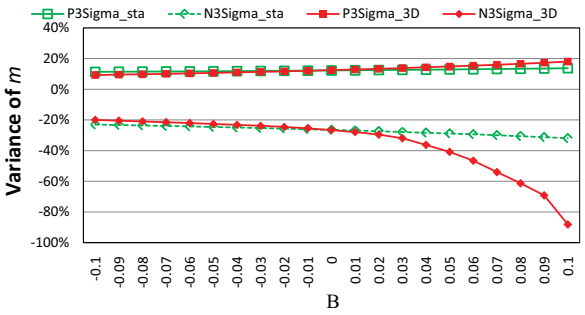

Fig. 16. Model with error coefficient B.

expected, the simulation results show that a larger correlation results in a smaller G variation. When the two memristors are fully correlated (means they are identical), we still observe $\sim \pm 2.8\%$ variation. This small variations come from the intrinsic total memristance variations of the two memristors and cannot be canceled to each other at circuit design level.

C. Model error tolerance analysis

Our previous analysis was build on the polynomial representation or Gaussian distribution assumption on the physical parameters of TiO_2 memristors. However, ignoring higher order approximation in our model may incur inaccuracy when the variation is large. As an example, ionic drift in a TiO_2 memristor has an exponential relationship with the applied electrical field [15]. Our previous linear approximation may not accurately describe the doping front movement when the applied voltage is large.

Based on Taylor expansion, a higher order relationship (e.g., the second order term) can be added on top of Eq. (3). The modified velocity of doping front movement $v(t)$ becomes

$$v(t) = \frac{d\alpha}{dt} = \mu_v \cdot \frac{R_L}{h^2} \cdot \frac{V(t)}{M(\alpha)} + B \cdot .(\frac{V(t)}{M(\alpha)})^2. \qquad (20)$$

Here the coefficient B stands for the second order impact of the voltage/current on doping front movement, which is independent to other process variations. The normal value of B is between $[-0.1, 0.1]$ [15]. We take the exponential model of doping front movement in 3D Monte-Carlo simulation and replace the velocity express Eq. (3) with Eq. (20) in our statistical model, The comparison between the simulation results of both approaches for the variance of M is shown in Fig. 16.

As we can see from the simulation results, our statistical model companies well with the 3D device model when B is less than 0.04. When B is larger than 0.04, the results start to diverge due to the increased weight of the higher order term. Higher order approximation will help alleviate this issue at the cost of model complexity and run time increase.

VI. Conclusion

In this work, we developed a statistical model for TiO_2 thin-film memristors based on the theoretical understanding of the impact of process variations. The corresponding parameter extraction strategy and implementation considerations are also discussed. Simulation results show that our proposed statistical model has excellent accuracy and significantly reduced runtime cost: $3 \sim 4$ magnitudes run time reduction and only $\sim 2\%$ accuracy degradation are achieved compared to the existing device-based Monte-Carlo simulations. An application of memristor based op-amp VGA is also explored with our model.

References

[1] L. Chua. Memristor-the missing circuit element. *IEEE Transaction on Circuit Theory*, 18:507–519, 1971.

[2] D. B. Strukov, G. S. Snider, D. R. Stewart, and R. S. Williams. The missing memristor found. *Nature*, 453:80–83, 2008.

[3] D. Niu, Y. Chen, C. Xu, and Y. Xie. Impact of process variations on emerging memristor. In *Design Automation Conference (DAC)*, pages 877–882, 2010.

[4] Y. Ho, G. M. Huang, and P. Li. Nonvolatile memristor memory: device characteristics and design implications. In *International Conference on Computer-Aided Design*, pages 485–490, 2009.

[5] D. Strukov, J. Borghetti, and S. Williams. Coupled ionic and electronic transport model of thin-film semiconductor memristive behavior. *SMALL*, 5:1058–1063, 2009.

[6] Y. V. Pershin and M. D. Ventra. Experimental demonstration of associative memory with memristive neural networks. In *Nanotechnology Nature Proceedings*, page 345201, 2009.

[7] H. Choi, H. Jung, J. Lee, J. Yoon, J. Park, D.-J. Seong, W. Lee, M. Hasan, G.-Y. Jung, and H. Hwang. An electrically modifiable synapse array of resistive switching memory. *Nanotechnology*, 20(34):345201, 2009.

[8] A. Asenov, S. Kaya, and A. R. Brown. Intrinsic parameter fluctuations in decananometer MOSFETs introduced by gate line edge roughness. *IEEE Transaction on Electron Devices*, 50:1254–1260, 2003.

[9] D. Batas and H. Fiedler. A memristor SPICE implementation and a new approach for magnetic flux controlled memristor modeling. *IEEE Transactions on Nanotechnology*, 10:250-255, 2010.

[10] Y. Chen and X. Wang. Compact modeling and corner analysis of spintronic memristor. In *IEEE/ACM International Symposium on Nanoscale Architectures (NANOARCH)*, pages 7–12, July 2009.

[11] R. E. Pino, J. W. Bohl, N. McDonald, B. Wysocki, P. Rozwood, K. A. Campbell, A. Oblea, and A. Timilsina. Compact method for modeling and simulation of memristor devices: Ion conductor chalcogenide-based memristor devices. In *IEEE/ACM International Symposium on Nanoscale Architectures (NANOARCH)*, pages 1–4, 2010.

[12] M. Hu, H. Li, Y. Chen, X. Wang, and R. Pino. Geometry variations analysis of tio$_2$ thin film and spintronic memristors. In *Asia and South Pacific Design Automation Conference (ASP-DAC)*, pages 25–30, 2011.

[13] T. Wey and W. Jemison. Variable gain amplifier circuit using titanium dioxide memristors. *IET Circuits, Devices & Systems*, 5:59–65, 2011.

[14] Y. Pershin and M. Di Ventra. Practical approach to programmable analog circuits with memristors. *Circuits and Systems I: Regular Papers, IEEE Transactions on*, 57(8):1857–1864, 2010.

[15] D. Strukov and R. Williams. Exponential ionic drift: fast switching and low volatility of thin-film memristors. *Applied Physics A: Materials Science & Processing*, 94(3):515–519, 2009.